

Research Article

Amphibious Study on a Basilisk Lizard Inspired Robot

Jinjun Rao, Shuwen Cai, Fulong Xiao and Junxing Feng

Department of Mechatronics Engineering and Automation, Shanghai University, Shanghai 200072, China

Abstract: This study describes the amphibious study of a novel robot, which attempts to emulate the basilisk lizard's ability to run on the surface of water and walk on land. Functionally, the robot uses four bar mechanism as its driving leg with a self-adaptive foot added to its end. Through some hydromechanics calculations and analyses, its water running ability is theoretically verified. And via terrestrial gait planning, the feasibility of land walking is also realized and the performance has been tested by both simulation and experiment. This study opens the door for legged robots to become ambulatory over both land and water in China and its research method has given a good reference for further study of the amphibious robot.

Keywords: Amphibious, basilisk lizard, legged robot, reference

INTRODUCTION

With the continuous development of robotics and bio-science, study of the amphibious robots has become more and more popular. Amphibian animals, as a transition from aquatic to terrestrial vertebrates, inherit the dual characteristics of both aquatic and terrestrial vertebrates. They are not only endowed with the abilities of crawling on land like terrestrial vertebrates which are capable of obstacle crossing, but also possess the excellent performances of water swimming and running like aquatic vertebrates (Rui *et al.*, 2009). Till now, achievements of the amphibious robots have mostly been focused on the study of their driving mechanism. The development of computer science has offered a chance to test the feasibility of the designs through simulation, which is both time-saving and economical.

As is known to all, unlike small and lightweight animals, large creatures cannot reside at rest atop the water. They must strike the free surface with sufficient vigor to generate hydrodynamic forces on their driving legs capable of bearing their weight. Like most large animals, the basilisk lizard rely on a combination of form drag, added mass and gravitational forces generated by vigorous slapping of the free surface for both weight support and propulsion (John and David, 2006). By examining the surface locomotion of the basilisk lizard and elucidating their subtle water-walking technique Glasheen and McMahon characterized the driving stroke in terms of three distinct phases: slap, stroke and recovery (Tonia and Gorge, 2004).

Our study is mainly focused on the amphibious design and performance analysis of a basilisk lizard

inspired robot. On the basis of the preliminary researches and in the study of hydromechanics theory, an amphibious robot which can move both on land and water was brought forward. The knowledge gained by this research will help expand the limits of legged robot locomotion and also assist to increase the understanding of the basilisk lizard and its ability to walk in amphibious environment.

MODELING AND ANALYSIS OF THE ROBOT BASED ON WATER RUNNING

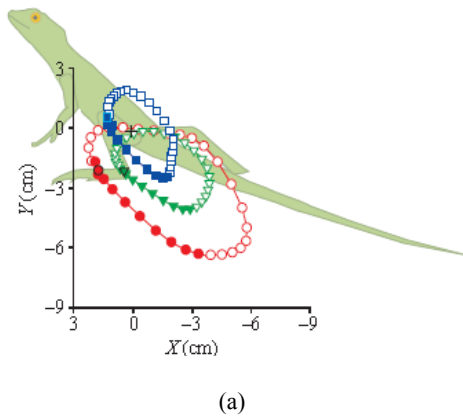
Selection of the driving mechanism: Since the real motion trajectory of a basilisk is elliptical as shown in Fig. 1a, Steven Floyd from Carnegie Mellon University found that a four bar mechanism in a Grashof crank-rocker configuration could mimic the motion of a basilisk's leg (Steven and Metin, 2008). Figure 1b presents a four bar mechanism and its resultant loop. A simplified foot is added to its end to make its simulative motion result seen more clearly. Given the simplicity and flexibility of the four bar mechanism, the configuration was used as a reference in our design.

Design of robot's feet: One can see from Fig. 1b that the simulative trajectory of a four bars mechanism is divided into four phases: $O \rightarrow A$, $A \rightarrow B$, $B \rightarrow C$ and $C \rightarrow O$. When the driving motor rotates a circle, hydro-forces acting on one foot corresponding to each phrase are analyzed in Fig. 2 where F_d and F_l are defined as the drag force and lift force, respectively.

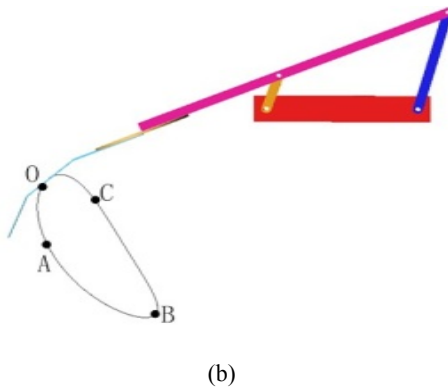
Obviously, averaged over time, the total lift of the system composed by F_d and F_l must equal the weight of

Corresponding Author: Jinjun Rao, Department of Mechatronics Engineering and Automation, Shanghai University, Shanghai 200072, China

This work is licensed under a Creative Commons Attribution 4.0 International License (URL: <http://creativecommons.org/licenses/by/4.0/>).



(a)



(b)

Fig. 1: Trajectories of the basilisk and simulation (Tonia and George, 2003)

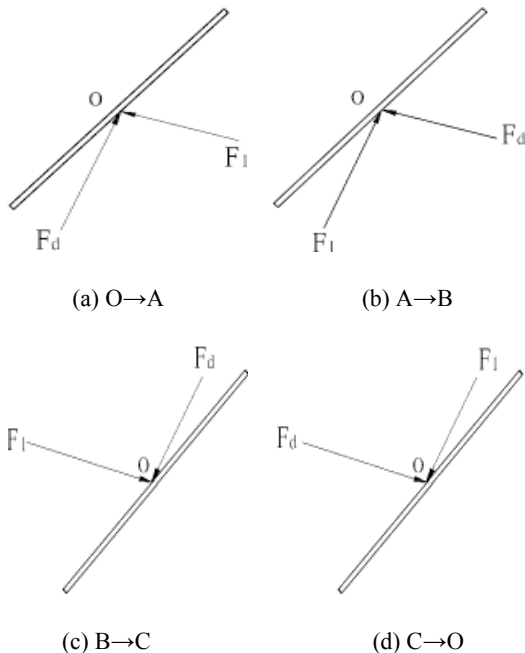


Fig. 2: F_1 and F_d acting on one foot

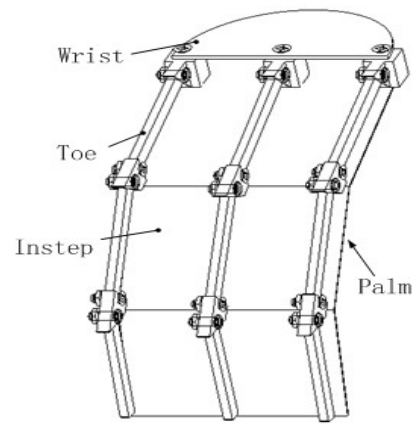


Fig. 3: Robot's self-adaptive foot

robot. From Fig. 2 one can conclude that the total lift is originated from the Phases $O \rightarrow A$ and $A \rightarrow B$. In other word, the total lift in Phase $O \rightarrow B$ benefits the stability of the robot for water-running while in Phase $B \rightarrow O$ it has the opposite effect. Inspired by the configuration of some water-paddling animals such as duck, a novel self-adaptive foot is brought forward (Shu-Wen *et al.*, 2012). This kind of foot contains a combination of three identical “toe” structures and a semi-circle “wrist” structure as seen in Fig. 3. Each “toe” consists of three stems with a hinge structure mounted between every two contiguous stems to constitute a revolute pair. A spring was added on each hinge and its contiguous later stem to ensure the upstream face is “palm” the moment foot contacting water. A piece of elastic material connected the fold joints are used to make up a compliant foot which can increase the effective spring stiffness of the flap bending. During Phase $O \rightarrow B$, the direction of the total lift force acting on the “palm” of foot is upward and the foot opens naturally leading to the increase of the total area of its upstream face. As a result, the total lift increases afterwards, bringing in the stability of the system advanced. During Phase $B \rightarrow O$, the upstream face is “instep” and all the effects brought by the total lift acting on the foot are contrary to the precedent, the foot closes naturally.

Overall modeling of the robot: As the quadrupedal robot shows higher stability than a bipedal one, the quadrupedal structure was applied. Furthermore, the total weight of the body should be limited within a certain range to meet the requirements of water running. Increased mass that the legs can lift is, of course, a positive aspect, whereas the increased power used is negative. Therefore, most parts of the body were frame structured and micro-motors were used to reduce the total weight.

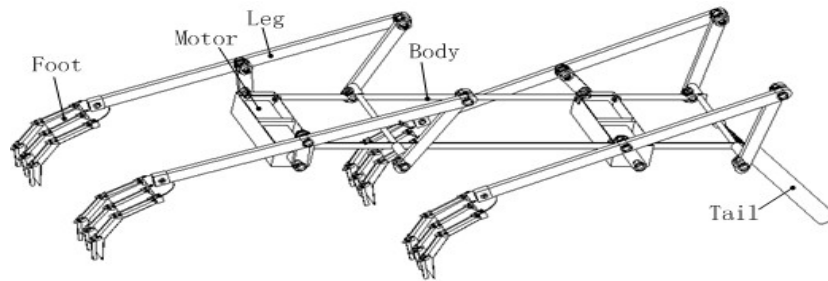


Fig. 4: Overall modeling of the robot

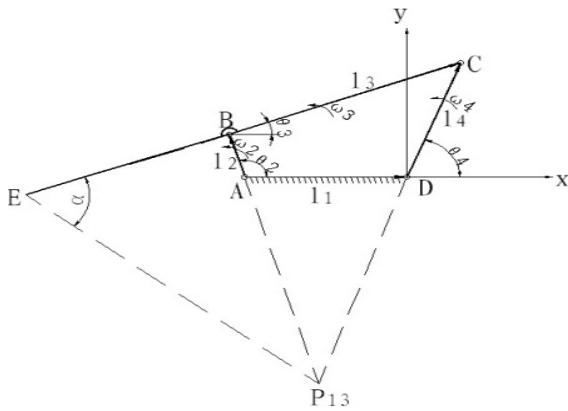


Fig. 5: Kinematics analysis of driving mechanism

After the preliminary modeling, several feasible analyses on water running were done to modify and optimize the original structure. As both F_d and F_l are proportional to v^2 , then for a robot with fixed weight, to increase the actuating speed v of the driving motors is a good means to rise the total lift. To realize water motion, the configuration of the robot must not only meet the requirements of lift but also satisfy the demand for water dynamic stability. That is to say, one must concern with the moment balance in both force-and-aft and left-to-right directions when the robot is running on water.

Considering the moment balance in force-and-aft direction, the resultant of F_d and F_l is divided into two components, one is a lift force F_{Lift} in the fluctuation direction to maintain the body of the robot and the other is a thrust force F_{Thrust} in the anteroposterior direction to push the body forward. Since the self-adaptive foot is applied, the values of F_{Lift} and F_{Thrust} are different even when the foot is in the locations the same distance from the surface of water in Phase O→B and Phase B→O. Result shows that as the clockwise resultant moment of Phase O→B is bigger than the anticlockwise resultant moment of Phase B→O, each leg of the robot has a tendency to drive the rear of robot into the river. To solve the above problem, a tail is placed at the back of

the body which can generate an anticlockwise moment to counteract part of the surplus clockwise moment, making the body stay upright while running on water. Since the moment generated by its two left-sided legs and the corresponding right-sided ones are equal in value and opposite in direction, the moment balance in the left-to-right direction is self-established. Thus far, the robot is capable of the ability to realize its water dynamic stability after structural modifications and its final configuration is shown in Fig. 4.

Actuating speed for water running: As the structure of this robot is confirmed, the chief concern of a free running system is its total lifting ability. As is said above, averaged over time, the total lift of the system must equal the weight of the robot. Unlike quadrupedal walking on land, where the weight is distributed over two or three legs (depending on the gait), when water running, only one leg is producing the majority of the total lift force F_{Lift} at a given time (Steven and Metin, 2008). Each leg, therefore, provide a peak lift force greater than the body weight. As is seen from Fig. 2, F_{Lift} is mostly generated in Phase O→B, thus during Phrase O→B the peak value of F_{Lift} must be greater than the body weight G .

As the total lift for water running is decided by the velocity of a single leg and the movement of the leg is generated by the actuating facility, thus the total lift on each foot is determined by the corresponding actuating speed of motor connecting with driving joint all in all. Figure 5 is a kinematics modeling of the driving mechanism where Crank AB acts as the driving part. Assuming the lengths of the Links 2~4 constituted the mechanism are $l_2 \sim l_4$ respectively and the homologous inclined angles are $\theta_2 \sim \theta_4$ relative to the coordinate axis x . Point P_{13} is the instant center of ground (Link 1) and Link 3. Point E is the mass center of one foot and the distance between Point B and E is l_5 . Through kinematics modeling, the numerical relationship between the actuating speed and its corresponding total lift is finally obtained.

From the closed vector equation $\vec{l}_1 + \vec{l}_4 = \vec{l}_2 + \vec{l}_3$, one can get the relationship between ω_2 and ω_3 :

$$\omega_3 = -\omega_2 l_2 \sin(\theta_2 - \theta_4) / [l_3 \sin(\theta_3 - \theta_4)] \quad (1)$$

Assuming the included angle between \vec{EC} and $\vec{P_{13}E}$ is α , the distance between instant center P_{13} and Point E is as follows:

$$\overline{P_{13}E} = \frac{\overline{EC} \sin(\theta_4 - \theta_3)}{\sin(\theta_4 - \theta_3 + \alpha)} \quad (2)$$

Since the thickness of the foot in this study is far less than its length, the relative motion between foot and water can be regarded as “flow around a flat plat at high attack angles”. So the peak value of the total lift should satisfy the following formula:

$$F_{Liftmax} = \max \left[\sin^2(\gamma - \theta_3) \rho u^2 \sin \gamma A + 12 \sin^2 \left(\frac{\gamma - \theta_3}{2} \right) \rho u^2 \cos \gamma A \right] > G \quad (3)$$

Combining the Eq. (1) to (3) and the existing relational expression $\gamma = 90^\circ - \alpha + \theta_3$ together, one can determine the critical actuating speed ω_{dmin} as follows:

$$\omega_{dmin} = \frac{\sqrt{\frac{G}{\left[\cos^2 \alpha \cos(\theta_3 - \alpha) - \frac{1}{2} \sin 2\alpha \sin(\theta_3 - \alpha) \right] \rho A}}}{\min(\overline{PE}) l_2 \sin(\theta_2 - \theta_3)} l_3 \sin(\theta_3 - \theta_4) \quad (4)$$

ANALYSIS AND REALIZATION OF THE ROBOT BASED ON LAND WALKING

Study of the terrestrial kinematics: In this study, each leg of the robot has only one driving joint. And every

time when it rotates, it affects the displacements of the body in both forward and fluctuation directions. The forward displacement can force the body to move ahead while the fluctuation of the body may result in the instability of the motion. Hence, if the robot moves fast, it is rather difficult to satisfy the requirements for stability in both directions that only terrestrial movement with a low speed is addressed here.

Like other quadrupedal robots, our basilisk lizard robot also walks with a time-varying topological structure. When one leg sways, the whole system shows an open chain structure and when all the legs contacting the ground, it turns to be a paralleled closed chain structure of multiple degrees. The result of its motion changes with the difference in landing points.

Assuming the robot is walking at a low speed and when the body of the robot walks a distance of Δx , the rotational angle $\Delta\theta$ of the driving joint in its homologous supporting leg can be determined via inverse kinematics in Fig. 5 with the following Eq. (5) to (6):

$$\left. \begin{aligned} l_1 + l_4 \cos \theta_4 &= l_2 \cos \theta_2 + l_3 \cos \theta_3 \\ l_4 \sin \theta_4 &= l_2 \sin \theta_2 + l_3 \sin \theta_3 \end{aligned} \right\} \quad (5)$$

$$\left. \begin{aligned} x_E &= l_2 \cos \theta_2 + l_3 \cos(\theta_2 + \theta_3) \\ y_E &= l_2 \sin \theta_2 + l_3 \sin(\theta_2 + \theta_3) \end{aligned} \right\} \quad (6)$$

Theoretical analysis of land walking stability:

Generally, when a robot walks in the static stable state its duty factor β always equals to or above 0.75, so at any moment, there are at least three legs to constitute a supporting polygon as shown in Fig. 6 where Point C is the center of ground reaction forces R_a, R_b, R_c acting at contacting points P_a, P_b, P_c respectively in a plane. Define the axis c_3 normal to the plane and let $\underline{F}_G, \underline{M}_G$

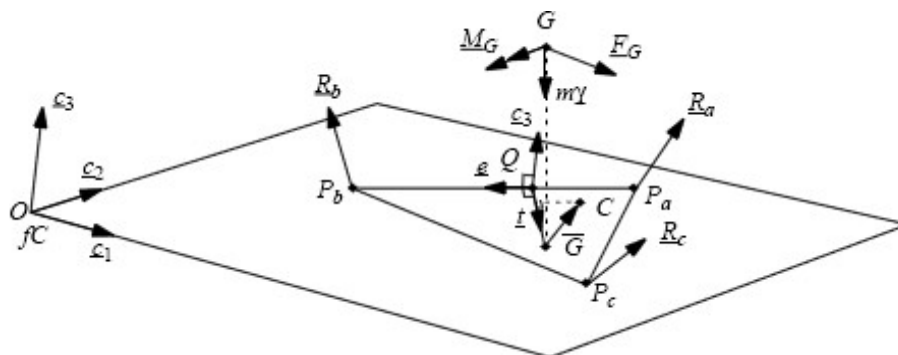


Fig. 6: Stability analysis of land walking (Hardarson, 2002)

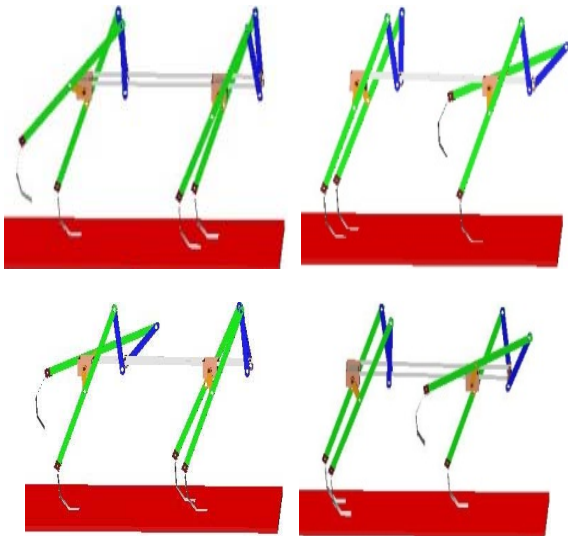


Fig. 7: Simulative motion in the order of 1-4-2-3

be the resultant force and moment respectively acting on the body. For a robot whose total mass is m , use \underline{r} as the gravity vector, the coordinate of Point C (Wang, 2007) is decided:

$$\underline{r}^{oc} = \underline{r}^{og} + \frac{c_3 \times (\underline{M}_G + \underline{r}^{g-g} \times \underline{F}_G)}{(c_3 \cdot (\underline{F}_G + m\underline{\gamma}))} \quad (7)$$

From the Eq. (7), one can see that the location of Point C is influenced by many factors and is changeable with time. Hence, there exists possibility that sometime Point C lands rightly at one edge of the supporting polygon, then the body is actually supported by two legs making up the edge line and the others can be regarded as “virtual” ones for the reason that they are ineffective for supporting. Obviously, the robot is unstable on this condition, even a rather small external force or moment can result in its deviation from the current state. So in order to make the robot walk stably, the center of ground reaction forces must be within the polygon at any time. Therefore, the robot must walk via its three or four legs supporting the body alternatively with its stability margin $S > 0$ and the duty factor $\beta > 0.75$ (Gao and Bingcong, 1992).

Gait planning of land walking: An ideal gait planning can realize the final posture of the robot completely the same as its original state after a step. Generally, as to a quadrupedal robot, the gaits of its four legs are defined similar to each other with the only difference in phases. In this study, every step of the robot is generated by the

rotational joints in its legs. Since the rotational angle of each leg is not always the same, the posture of each leg is different from one another. Under this circumstance, the relative forward displacement of each leg is diverse from each other even when the driving motors rotating a same angle. As the difference of synchronous rotational angles among the supporting legs is quite tiny, the error is neglected here. That the relative span E of each swinging legs equals in value is made as prerequisite for this gait planning.

As to land walking, there is no need for the foot to open or close, the included angle between every two stem is made fixed. A simplified model of the robot is established with each leg numbered 1~4 from left-front to right-back. The stability of a robot performs best while its legs swaying in the order 1-4-2-3 (Gao and Bingcong, 1992). Assuming that the rotational angle of each supporting leg is a uniform value θ during three-leg-supporting period and 2θ during four-leg-supporting period and then the rotational angle during swinging period is $360^\circ - 7\theta$. If the negative sign is used to express the rotational direction of a driving motor that makes the body backwards, then the original positions of each leg marked 1-4 are determined as follows respectively: $3\theta, -\theta, -4\theta, 0^\circ$, each relative to its own lowest point in the motion trajectory.

Simulative motion and parametric analysis: To verify the accuracy of planned gait for land walking and optimize the performance of the designed robot, a virtual prototype was developed. Before simulative motion, static and dynamic friction coefficients were set to 0.3 and 0.5 and θ , the rotational angle of supporting legs during three-leg-supporting period was set to 10° . Process of simulative motion is shown in Fig. 7.

After simulation, a successive of analyses was done to reinforce the feasibility of planned gait. Figure 8 shows that the curves of each leg’s displacement in the forward direction are resemble in shape during a single pass which is well accordant with our original intention for gait planning.

As in a unchangeable simulative condition, we wished to know if there was an optimum value of a motor’s rotational angle θ or stride frequency f . Set the value of stride frequency fixed with the value of rotational angle θ ranging from 8° to 12° , one can get that a larger rotational angle leads to larger body fluctuation as seen in Fig. 9, but larger rotational angle also leads to larger forward displacement seen in Fig. 10. As the mass center of the robot is 130 mm up from the ground in the design and generally the body

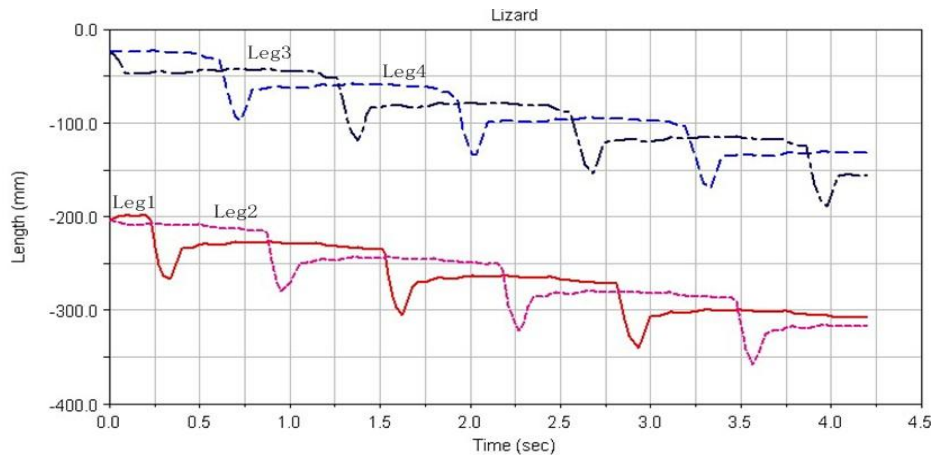


Fig. 8: Movement of each leg

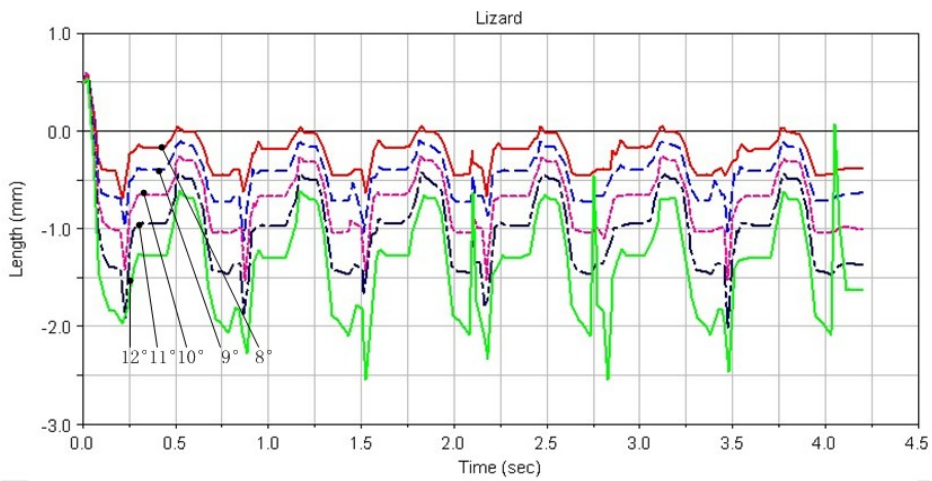


Fig. 9: Fluctuation curves under different driving angles

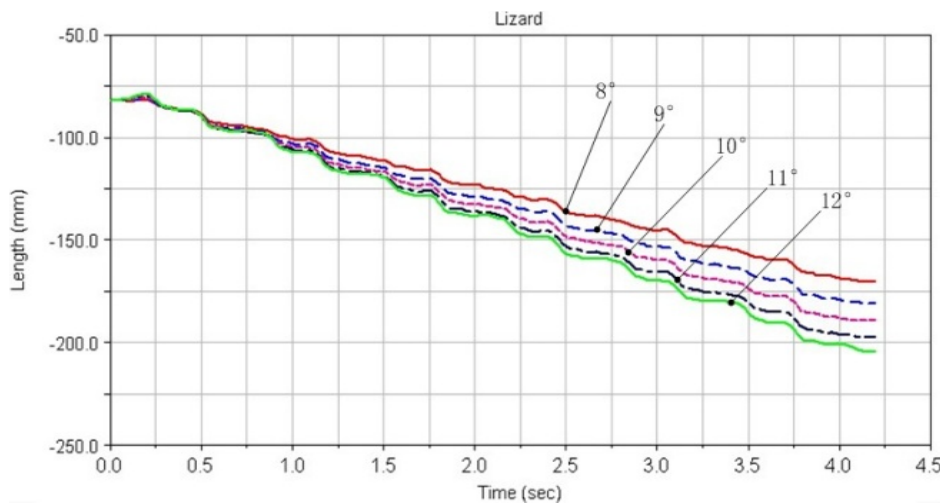


Fig. 10: Forward displacement curves under different driving angles

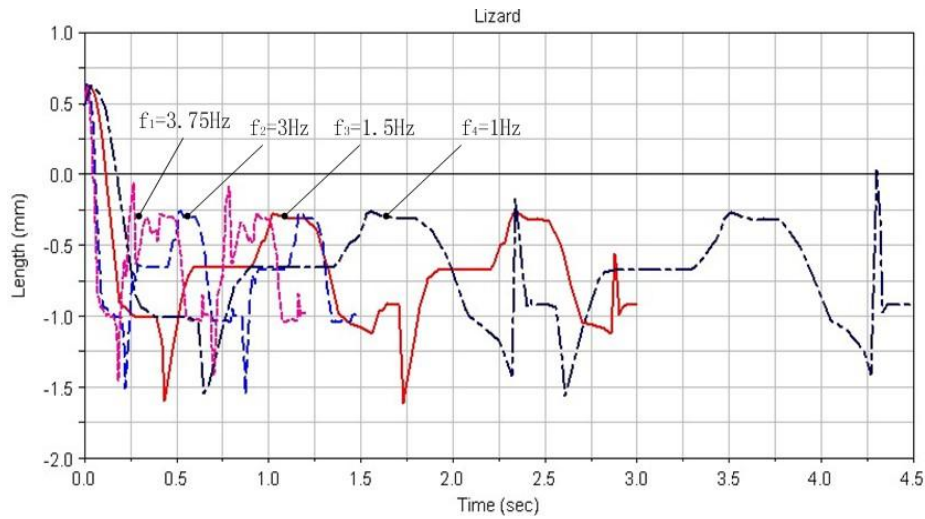


Fig. 11: Fluctuation curves at different swaying frequencies

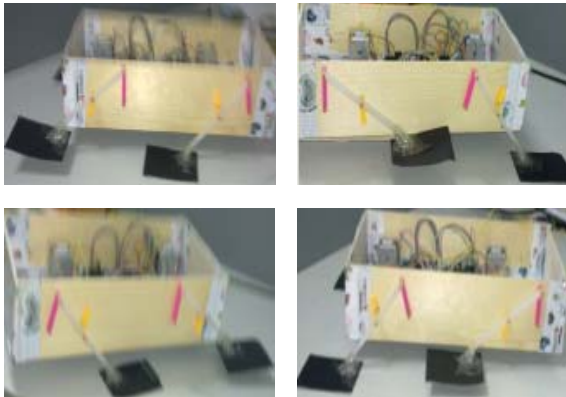


Fig. 12: Robot's movement in the order of 1-4-2-3

fluctuation ratio of a legged robot during the stable walking state should not exceed 1%, hence $\theta = 10^\circ$ is decided as the optimum value of rotational angle of supporting legs during three-leg-supporting period in the given condition. Figure 11 shows that as θ is fixed to 10° , when the stride frequency is lower or equals to 3 Hz, difference in body fluctuation is tiny, but when the value of stride frequency continuous to grow there exists a radical change in body fluctuation. Since a larger frequency leads to higher performance, here $f = 3$ Hz is chosen as the optimum value of stride frequency.

Experiment on land walking: Experiment of the robot walking on land was performed as a complement to test the simulation results. A quadrupedal simplified robot was established 400 mm in length, 100 mm in width and 10 mm in height with four identical crank-rocker configurations making up its driving legs as seen in

Fig. 12. Four DC motor were put inside the body to actuate the driving joints. Since this experiment here was only done on the ground, from the view of simplicity for operation, its self-adaptive feet were replaced by some rubber chucks with a piece of black paper pasted to the surface of each piece, making the results seen more clearly. During the experiment, one could see that the robot walked stably at a low speed. In the process, Parameter E, the relative stride span of a leg was measured 12 mm and Parameter λ , a step length of the robot was 17 mm. The result $E < \lambda$ satisfied the requirement of a quadrupedal robot walking in the static stable state, which successfully added the veracity and rationality of the planned gait.

CONCLUSION

In this study, an amphibious basilisk lizard inspired robot is designed. A novel self-adaptive foot based upon the water running ability is modeled. Using four bar mechanism, the robot can move in amphibious environment theoretically. The work not only opens a door but also gives a good reference for the study of bipedal and quadruped robots becoming ambulatory over both land and water. Up to now, ability of the robot to walk on land has already been tested by both simulation and experiment while its ability of water running hasn't been examined experimentally yet. Doing water experiment is rather difficult that it shows far higher demands on both quality of experimental facilities and researchers.

Future study will towards the test and verification of the ability for water running. Some preliminary preparations have already been done for water

experiment. During the process, some real values of water motion parameters aim to obtain on basis of the theoretical analyses.

ACKNOWLEDGMENT

The authors wish to thank the helpful comments and suggestions from my teachers and colleagues in the Department of Precision Mechanical Engineering of Shanghai University. This research is jointly sponsored by State Leading Academic Discipline and Shanghai Leading Academic Discipline and National Natural Science Foundation of China under Grant 50905103, the Graduate Innovation Fund of Shanghai University (No. SHUCX120077).

REFERENCES

- Gao, F. and C. Bingcong, 1992. A method of gait design of quadruped walking vehicle-the method of critical states. *Chines J. Mech. Eng.*, 28(5): 740-741.
- Hardarson, F., 2002. Stability analysis and synthesis of statically balanced walking for quadruped robots. Ph.D. Thesis, Royal Institute of Technology, Stockholm, Sweden, pp: 25-30.
- John, W.M.B. and L.H. David, 2006. Walking on water: Biocomotion at the Interface. *Annu. Rev. Fluid. Mech.*, 38: 339-369.
- Rui, D., Y. Junzhi, Y. Qinghai and T. Min, 2009. Kinematics modeling and simulation for an amphibious robot: Design and implementation. *Proceeding of the IEEE International Conference on Automation and Logistics, Shenyang*, pp: 35-40.
- Shu-Wen, C., R. Jin-Jun and X. Fu-Long, 2012. Foot design of a basilisk lizard inspired robot on water. *Mach. Des. Res.*, 28(1): 22-25.
- Steven, F. and S. Metin, 2008. Design and development of the lifting and propulsion mechanism for a biologically inspired water runner robot. *IEEE T. Rbot.*, 24: 698-709.
- Tonia, S.H. and V.L. George, 2003. Three-dimensional hindlimb kinematics of water running in the plumed basilisk lizard (*Basilisk plumifrons*). *J. Ex. Biol.*, 206: 4363-4377.
- Tonia, H.S. and V.L. George, 2004. Running on water: Three-dimensional force generation by basilisk lizards. *PNAS*, 101(48): 16784-16788.
- Wang, P., 2007. Research on quadruped robot steadily walking planning and controlling technology. Ph.D. Thesis, Harbin Institute of Technology, Harbin, China, pp: 29-30.